JOURNAL OF
Applied Polymer
SCIENCE

Special Issue: Polymers for Microelectronics

Guest Editors: Dr Brian Knapp (Promerus LLC) and
Prof. Paul A. Kohl (Georgia Institute of Technology)

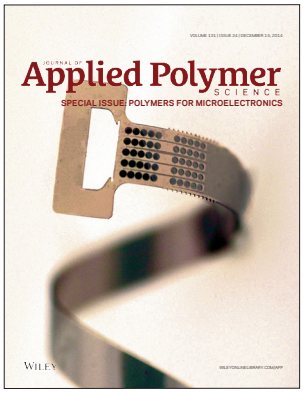

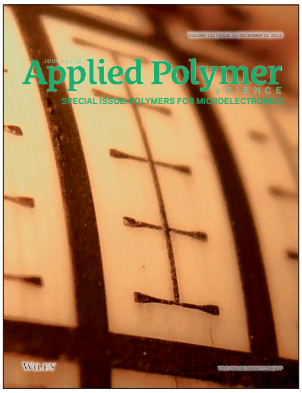

EDITORIAL

Polymers for Microelectronics
B. Knapp and P. A. Kohl, *J. Appl. Polym. Sci.* 2014, **DOI: 10.1002/app.41233**

REVIEW

Negative differential conductance materials for flexible electronics
A. Nogaret, *J. Appl. Polym. Sci.* 2014, **DOI: 10.1002/app.40169**

RESEARCH ARTICLES

Generic roll-to-roll compatible method for insolubilizing and stabilizing conjugated active layers based on low energy electron irradiation
M. Helgesen, J. E. Carlé, J. Helt-Hansen, A. Miller, and F. C. Krebs, *J. Appl. Polym. Sci.* 2014, **DOI: 10.1002/app.40795**

Selective etching of polylactic acid in poly(styrene)-block-poly(D,L)lactide diblock copolymer for nanoscale patterning
C. Cummins, P. Mokarian-Tabari, J. D. Holmes, and M. A. Morris, *J. Appl. Polym. Sci.* 2014, **DOI: 10.1002/app.40798**

Preparation and dielectric behavior of polyvinylidene fluoride composite filled with modified graphite nanoplatelet
P. Xie, Y. Li, and J. Qiu, *J. Appl. Polym. Sci.* 2014, **DOI: 10.1002/app.40229**

Design of a nanostructured electromagnetic polyaniline–Keggin iron–clay composite modified electrochemical sensor for the nanomolar detection of ascorbic acid
R. V. Lilly, S. J. Devaki, R. K. Narayanan, and N. K. Sadanandhan, *J. Appl. Polym. Sci.* 2014, **DOI: 10.1002/app.40936**

Synthesis and characterization of novel phosphorous-silicone-nitrogen flame retardant and evaluation of its flame retardancy for epoxy thermosets
Z.-S. Li, J.-G. Liu, T. Song, D.-X. Shen, and S.-Y. Yang, *J. Appl. Polym. Sci.* 2014, **DOI: 10.1002/app.40412**

Electrical percolation behavior and electromagnetic shielding effectiveness of polyimide nanocomposites filled with carbon nanofibers
L. Nayak, T. K. Chaki, and D. Khastgir, *J. Appl. Polym. Sci.* 2014, **DOI: 10.1002/app.40914**

Morphological influence of carbon modifiers on the electromagnetic shielding of their linear low density polyethylene composites
B. S. Villacorta and A. A. Ogale, *J. Appl. Polym. Sci.* 2014, **DOI: 10.1002/app.41055**

Electrical and EMI shielding characterization of multiwalled carbon nanotube/polystyrene composites
V. K. Sachdev, S. Bhattacharya, K. Patel, S. K. Sharma, N. C. Mehra, and R. P. Tandon, *J. Appl. Polym. Sci.* 2014, **DOI: 10.1002/app.40201**

Anomalous water absorption by microelectronic encapsulants due to hygrothermal-induced degradation
M. van Soestbergen and A. Mavinkurve, *J. Appl. Polym. Sci.* 2014, **DOI: 10.1002/app.41192**

Design of cyanate ester/azomethine/ZrO_2 nanocomposites high-k dielectric materials by single step sol-gel approach
M. Ariraman, R. Sasi Kumar and M. Alagar, *J. Appl. Polym. Sci.* 2014, **DOI: 10.1002/app.41097**

Furan/imide Diels–Alder polymers as dielectric materials
R. G. Lorenzini and G. A. Sotzing, *J. Appl. Polym. Sci.* 2014, **DOI: 10.1002/app.40179**

High dielectric constant polyimide derived from 5,5'-bis[(4-amino) phenoxy]-2,2'-bipyrimidine
X. Peng, Q. Wu, S. Jiang, M. Hanif, S. Chen, and H. Hou, *J. Appl. Polym. Sci.* 2014, **DOI: 10.1002/app.40828**

The influence of rigid and flexible monomers on the physical-chemical properties of polyimides
T. F. da Conceição and M. I. Felisberti, *J. Appl. Polym. Sci.* 2014, **DOI: 10.1002/app.40351**

JOURNAL OF
Applied Polymer
SCIENCE

Special Issue: Polymers for Microelectronics

Guest Editors: Dr Brian Knapp (Promerus LLC) and
Prof. Paul A. Kohl (Georgia Institute of Technology)

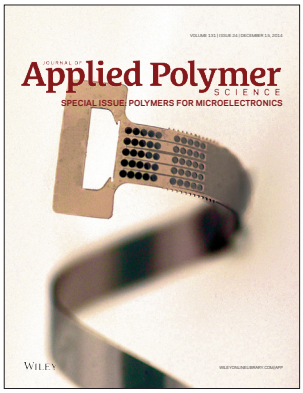

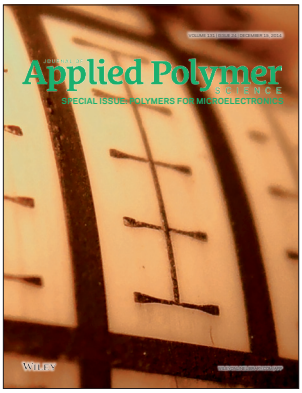

Development of polynorbornene as a structural material for microfluidics and flexible BioMEMS
A. E. Hess-Dunning, R. L. Smith, and C. A. Zorman, *J. Appl. Polym. Sci.* 2014, **DOI:** 10.1002/app.40969

A thin film encapsulation layer fabricated via initiated chemical vapor deposition and atomic layer deposition
B. J. Kim, D. H. Kim, S. Y. Kang, S. D. Ahn, and S. G. Im, *J. Appl. Polym. Sci.* 2014, **DOI:** 10.1002/app.40974

Surface relief gratings induced by pulsed laser irradiation in low glass-transition temperature azopolysiloxanes
V. Damian, E. Resmerita, I. Stoica, C. Ibanescu, L. Sacarescu, L. Rocha, and N. Hurduc, *J. Appl. Polym. Sci.* 2014, **DOI:** 10.1002/app.41015

Polymer-based route to ferroelectric lead strontium titanate thin films
M. Benkler, J. Hobmaier, U. Gleißner, A. Medesi, D. Hertkorn, and T. Hanemann, *J. Appl. Polym. Sci.* 2014, **DOI:** 10.1002/app.40901

The influence of dispersants that contain polyethylene oxide groups on the electrical resistivity of silver paste
T. H. Chiang, Y.-F. Chen, Y. C. Lin, and E. Y. Chen, *J. Appl. Polym. Sci.* 2014, **DOI:** 10.1002/app.41183

Quantitative investigation of the adhesion strength between an SU-8 photoresist and a metal substrate by scratch tests
X. Zhang, L. Du, and M. Zhao, *J. Appl. Polym. Sci.* 2014, **DOI:** 10.1002/app.41108

Thermodynamic and kinetic aspects of defectivity in directed self-assembly of cylinder-forming diblock copolymers in laterally confining thin channels
B. Kim, N. Laachi, K. T. Delaney, M. Carilli, E. J. Kramer, and G. H. Fredrickson, *J. Appl. Polym. Sci.* 2014, **DOI:** 10.1002/app.40790

Journal of Applied Polymer Science

Polymer-Based Route to Ferroelectric Lead Strontium Titanate Thin Films

Manuel Benkler,[1] Jost Hobmaier,[1] Uwe Gleißner,[1] Anna Medesi,[1] Daniel Hertkorn,[1] Thomas Hanemann[1,2]

[1]Department of Microsystems Engineering, University of Freiburg, Georges-Köhler-Allee 102, D-79110 Freiburg, Germany
[2]Karlsruhe Institute of Technology, Institute for Applied Materials-Materials Process Technology, Hermann-von Helmholtz-Platz 1, D-76344 Eggenstein-Leopoldshafen, Germany
Correspondence to: M. Benkler (E-mail: manuel.benkler@imtek.uni-freiburg.de)

ABSTRACT: Ceramic films with high values of ferroelectricity, piezoelectricity, and dielectricity with perovskite structure, like lead zirconate titanate (PZT, $PbZr_xTi_{1-x}O_3$), lead strontium titanate (PST, $Pb_xSr_{1-x}TiO_3$), and barium strontium titanate (BST, $Ba_xSr_{1-x}TiO_3$), are subjects of intensive research due to their use in sensors, energy harvesters, capacitors, and FeRAMs. Here a novel, simple way to produce micropatterned perovskite PST thin films on silicon substrates by a polymer-based direct UV-lithography process is presented. By acrylic acid modification of PST precursor sols it is possible to generate photosensitive metal organic PST precursor xerogel films by spin-coating and subsequently drying on silicon wafers. These films can be patterned by UV-lithography and developed with organic solvents. The resulting patterned gel films can be crystallized in air via rapid thermal annealing. The obtained perovskite thin ceramic films are polycrystalline and fine grained. © 2014 Wiley Periodicals, Inc. J. Appl. Polym. Sci. **2014**, *131*, 40901.

KEYWORDS: films; irradiation; photopolymerization; thermogravimetric analysis; X-ray

Received 26 February 2014; accepted 21 April 2014
DOI: 10.1002/app.40901

INTRODUCTION

Because of their high values of ferroelectric polarization, piezoelectric coefficient, and dielectric permittivity ferroelectric films with perovskite structure like lead zirconate titanate ($PbZr_xTi_{1-x}O_3$, PZT), lead strontium titanate ($Pb_xSr_{1-x}TiO_3$, PST), and barium strontium titanate ($Ba_xSr_{1-x}TiO_3$, BST) films are widely used in the fields of sensors, energy harvesting, capacitors, and FeRAMs technology.[1–6] PST and BST films can be used for tunable microwave device components, such as phase shifters, filters, varactors, and delay lines.[7,8] PST thin films are promising candidates for these specific applications as PST thin films show lower loss tangent, larger tunability, and lower processing temperatures than BST thin films.[9]

Many methods to produce PST thin films were reported. The films are deposited by different types of evaporation and sputtering techniques, for example, Pulsed Laser Deposition or RF Magnetron Sputtering.[9–12] Chemical solution deposition methods especially by sol-gel techniques have also been well investigated.[8,13–18] Sol-gel process offers the opportunity to produce very homogenous ceramic films. Due to the easy mixing of the starting materials during sol synthesis the stoichiometry of the films can simply be adjusted. This is another advantage especially for doped materials.

Patterning of PST films is only reported in combination with PZT as strontium doped PZT.[19] Leech et al. used a 5 ns pulsed eximer laser to pattern strontium doped PZT thin films that were deposited by RF magnetron sputtering. To our knowledge no other articles are dealing with micropatterning methods for pure PST films. But in fact almost all proven methods and processes to pattern other ferroelectric ceramic films like PZT films should be suitable for PST films as well. We have summarized these methods and processes in our earlier article about the micropattering of PZT thin films.[20]

An interesting alternative to these methods is provided by sol-gel chemistry. By photosensitive metal precursor sols it is possible to produce directly photopatternable green films, which can be converted to crystalline ceramic films by thermal treatment. Several additives that make a sol photosensitive were used for directly UV-photopatternable PZT films. Chemical modifiers like β-diketones (acetylacetone, benzoylacetone) give high photosensitivity to the sol.[21,22] Also *ortho*-nitrobenzaldehyde can be used as photoreactive compound.[23,24] For photopolymerizable monomers only few methods were reported.[25–27] Marson et al used a photosensitive PZT solution fabricated out of amorphous PZT powder, made by a sol-gel process, acrylic acid, and a sensitizer. Photosensitive films were produced by spin coating of

this solution and the obtained photosensitive films were patterned by UV-lithography. These green films were transformed to thick ceramic films by thermal treatment. The crystalline PZT films were up to 1.9 μm thick with a minimum feature size of 50 μm but show massive crack formation.[25,26] Chemical modification of precursor alkoxides and acetates with photopolymerizable monomers like methacrylic acid is another way to obtain photoreactive sols. Kololuoma et al. produced patterned PLZT (lanthanum-doped PZT) thin films by methacrylic acid modification of a precursor sol. The sol synthesis started with dissolution of acetate trihydrate and lanthanum acetate hydrate in methacrylic acid. The solution was stirred for 72 h, dehydrated by vacuum distillation and finally diluted with 2-isopropoxyethanol. A second solution containing zirconium and titanium alkoxides was obtained by dissolving the metal alkoxides in 2-isopropoxyethanol and stirring for 72 h to replace the propoxy and isopropoxy ligands with 2-isopropoxyethanol. Then, the solvents were removed by vacuum distillation. Finally, the lead lanthanum solution and a photoinitiator (Irgacure 819, Ciba) were added to this solution to get a UV-sensitive sol. To avoid the hydrolysis of used precursor alkoxides all steps of the synthesis were performed under N_2 atmosphere. Photosensitive sols were produced by spin coating on borosilicate and silicone substrates with a thin TiO_2 film. The films were patterned by contact UV-lithography with a photomask and developed after a post exposure bake with isopropanol. The green PLZT films were transformed to ceramic films in a 23 h annealing process with a maximum temperature of 630°C. Finally, patterned ceramic PLZT films with perovskite phase as well as a pyrochlore phase, a thickness of about 100 nm and a minimum feature size of about 30 μm were formed.[27]

In our previous article on fine patterned PZT thin films by direct UV-lithography we were able to present a less time consuming, much easier approach to produce UV-sensitive sols.[20] High photosensitivity was achieved by chemical methacrylic acid modification of the precursor alkoxides/acetates and the addition of an UV-initiator (diphenyl(2,4,6-trimethylbenzoyl)-phosphine oxide). UV-curable xerogel green PZT films were obtained by spin coating and drying. These films were patterned by UV-lithography using a maskaligner. The patterning process is based on a polymerization reaction of methacrylic acid–metal complexes in the irradiated areas induced by UV-lithography. This reaction decreases the solubility of the irradiated gel-film areas in organic solvents and so it can be used for a patterning process. The obtained green PZT films were transformed to fine patterned, crystalline PZT thin films with perovskite structure by rapid thermal annealing. Crack free films were about 50 nm thick with resolutions in the lower μm range (1–3 μm). Special attention was paid to the ease of the process. Even for the sol synthesis no sophisticated techniques like the use of inert gas atmosphere or dehydration of the sol by distillations were necessary.

Based on the gained knowledge a simple and easy polymer-based method to produce micropatterned PST thin films was developed. The simple single step lithography process is based on the chemical acrylic acid modification of a PST precursor sol which is acting like a negative photoresist. For optimal applicability, the sol synthesis was kept as simple as possible. No sophisticated techniques as the use of an inert gas atmosphere were used and no distillation steps to dehydrate the sol were necessary. Therefore, the presented process is much easier to handle and less time consuming than other known methods to produce UV-sensitive sols. UV-irradiation is able to start a radical polymerization reaction of the monomer metal precursor complexes of the synthesized sols. The resulting polymer metal matrix in the irradiated areas is less soluble in organic solvents than the monomer metal complexes in the not irradiated areas. This solubility difference is applied to a fine patterning process and so the sol is acting like a negative photoresist. The obtained PST green xerogel films can be transformed to the desired perovskite PST thin films by thermal annealing. Finely patterned crack free ceramic thin PST films are accessible by this simple polymer-based method using direct UV-lithography.

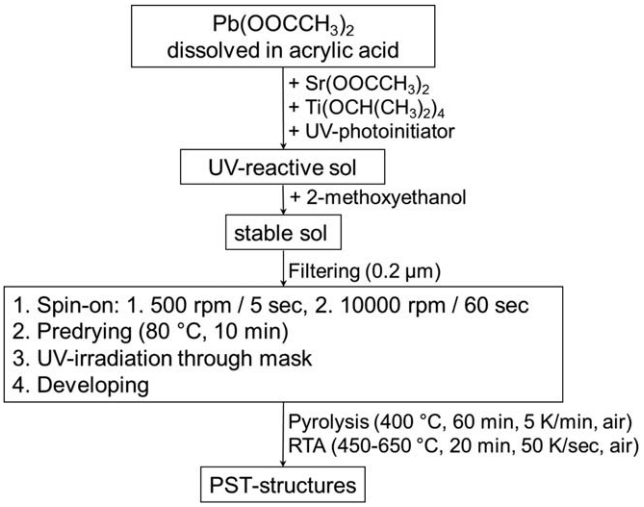

Figure 1. Flow chart of the UV-lithography process for patterned PST thin films.

EXPERIMENTAL

Sol Synthesis and Characterization

Figure 1 schematically shows the preparation and patterning process of the PST thin films. For the synthesis of the sol, the following chemicals were used as received from suppliers: lead(II) acetate trihydrate (99.0–130.0%, Alfa Aesar), strontium(IV) acetate hemihydrate (Reagent grade, Alfa Aesar), titanium(IV) isopropoxide (p.a., Merck), acrylic acid (AA, p.a., Merck), and 2-methoxyethanol (ME, 99.9%, Aldrich). Molar ratios were 0.4 : 0.6 : 1.0 : 3.4 : 19.0 for Pb, Sr, Ti, AA, and 2-methoxyethanol, respectively. The metal alkoxides and acetates were weighed out and mixed to give $Pb_{0.4}Sr_{0.6}TiO_3$ films. For an amount of 10 mL sol, the chemicals were mixed as follows: First, lead acetate trihydrate (0.72 g, 1.89 mmol) and strontium acetate hemihydrate (0.61 g, 2.84 mmol) were mixed into acrylic acid (1.15 g, 15.97 mmol). Then, titanate isopropoxide (1.35 g, 4.74 mmol) was added slowly to the solution. Afterwards the UV-photoinitiator (diphenyl(2,4,6-trimethylbenzoyl)-phosphine oxide, TCI, 0.032–0.32 g, 0.09–0.9 mmol) was added, the resulting stock solution was diluted with 2-methoxyethanol (6.85 g, 15.97 mmol) and stirred until a homogeneous light

yellow solution was obtained. The resulting solution was filtered with a membrane syringe filter (0.2 μm). Finally, the viscosity of the sol was measured by rheometry (Thermo Haake RheoStress 300), using a cone/plate system and shear rates of 10–1000 1/sec at 21°C.

Xerogel Film Fabrication and Characterization

Fabrication of the patterned PST xerogel films was carried out in a class 1000 clean room (temperature 21°C). Thin films were formed in a two stage spinning process onto Si-substrates (orientation 100). The sol was spread over the substrate for 5 sec at 500 rpm and then, spun-on for 30 sec at 10,000 rpm. After spin coating, the resulting films were dried on a hotplate at 80°C for 10 min. For the patterning process contact lithography with a photomask and UV-irradiation from a mercury UV-lamp source (9 mW/cm^2 at 365 nm) was used (Suess MA6). The lamp output is checked periodically by clean room service staff. The films were exposed for 10 min (UV dose: 5.4 J/cm^2) and without further treatment (no post bake etc.) developed with a mixture of ethyl acetate, 2-methoxyethanol, and methanol (volume ratio: 75 : 10 : 15) to obtain patterned PST xerogel films.

Ceramic Film Fabrication and Characterization

PST xerogel structures were first pyrolized at 400°C for 1 h (heating/cooling rate: 5 K/min) and then, sintered in ambient air by rapid thermal annealing (MILA-3000, ULVAC-RIKO) at different temperatures (450–650°C) for 20 min with a heating rate of 50 K/sec. The obtained patterned thin ceramic PST films were investigated by scanning electron microscopy (SEM), X-ray diffractometry, profilometry, and hysteresis measurements. The morphology and quality of the films was investigated by SEM (Phenom World, Phenom Pro Desktop SEM). Due to the operation mode of the Phenom Pro Desktop SEM the films could be investigated without further treatment like the deposition of a conductive layer. SEM pictures were taken using an acceleration voltage of 5 kV. The thicknesses of the films were measured by profilometry (Tencor P11) using a scanning speed of 200 µm/sec with a sampling rate of 50 Hz. Film composition and phase formation were investigated by X-ray diffractometry (Siemens D5000) with $CuK_{\alpha 1}$ radiation ($\lambda = 1.5406$ Å) in the 2θ range of 20 to 60° with steps of 0.02°. Hysteresis measurements were performed with a Radiant RT66B dielectric tester. For these measurements not patterned, crystallized films deposited on platinum plated silicon wafer were used. As top electrode a silver electrode painted with silver lacquer was used. The bottom Pt-electrode was wired to the tester by an alligator clip and the silver top electrode was connected by a contact spring. A bipolar voltage profile in the range of −2.5–2.5 V was chosen. The measurement was performed after a pre-loop (delay 100 ms) with the same settings with a hysteresis period of 100 ms.

RESULTS AND DISCUSSION

Sol Properties

Viscosities of the synthesized PST sols showed a significant dependence on the 2-methoxyethanol (ME) content (Figure 2). The viscosities of the sols were decreased with higher 2-methoxyethanol content and the diluted sols showed almost Newtonian behavior. The viscosity was reduced by 83 % in sols with a 2-methoxyethanol content of 50 vol %, in sols with 75 vol % ME about 92 %. So the increase of the 2-methoxyethanol content from 50 to 75 vol % lowered the viscosity of the sol by approximately 50 %. To obtain thin films only sols with higher 2-methoxyethanol content of 75 vol % were used for preparation of films presented in this article.

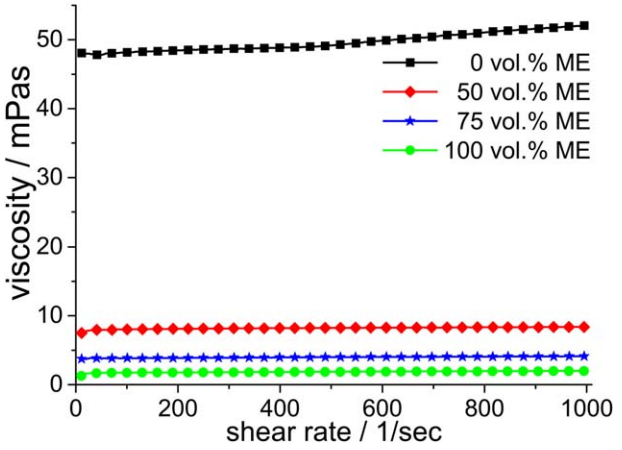

Figure 2. Influence of the 2-methoxyethanol (ME) content of the PST sols on the viscosity of the sols. [Color figure can be viewed in the online issue, which is available at wileyonlinelibrary.com.]

Patterning of Xerogel Green PST Films

Xerogel green PST films obtained by spin coating and drying of the sol showed UV-sensitivity. After UV-irradiation the green gel films were no longer soluble in some organic solvents. This change is a strong hint to structural changes in the films, most likely caused by a polymerization reaction of the acrylic acid. The suggested mechanism of the polymerization reactions is shown in Figure 3. In the first step, the UV-irradiation causes a decomposition of the UV-photoinitiator (diphenyl(2,4,6-trimethylbenzoyl)-phosphine oxide) into two radicals.[28] These radicals can start a radical polymerization reaction of the metal acrylates. The resulting polymers show different solubilities in variant organic solvents compared to the not polymerized (metal acrylate-) monomers. The observed solubility change between polymerized and not polymerized areas of the green film was applied to a fine patterning process. For this purpose, the xerogel green PST films were selectively irradiated with UV-light using a chrome glass mask and then developed in appropriate organic solvents. Because of the polymerization reaction the metal precursors are integrated in a polymer matrix and are stable fixed until the thermal annealing of the green film and the resulting formation of the ceramic film. So the developed PST sol can be processed like a commercial photoresist and is acting like a negative photo resist. To obtain good developed microstructures it is very important to have significant differences in the solubility between UV-irradiated and not irradiated areas. A development solution of ethyl acetate, 2-methoxyethanol, and methanol (volume ratio: 75 : 10 : 15) showed the best results. At room temperatures development times between 5–8 min were used.

Influence of Initiator Content

The influence of the UV-initiator content on the green film quality was investigated. If low initiator quantities (0.09 mmol)

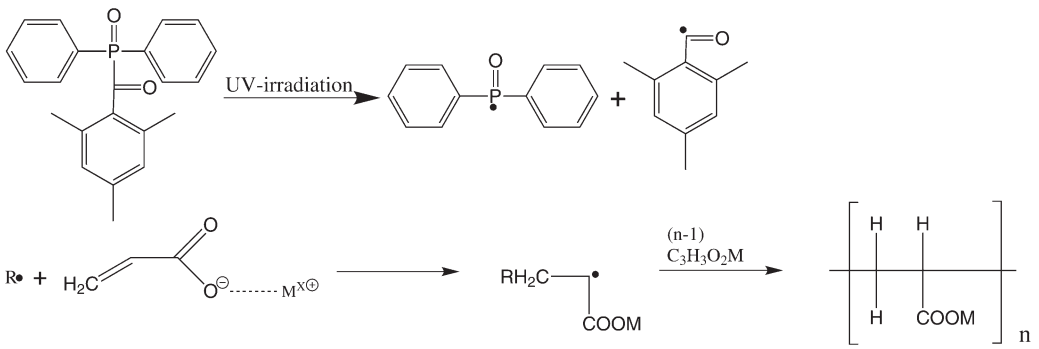

Figure 3. UV-light induced decomposition of the initiator and proposed mechanism of radical polymerization of metal acrylates.[28]

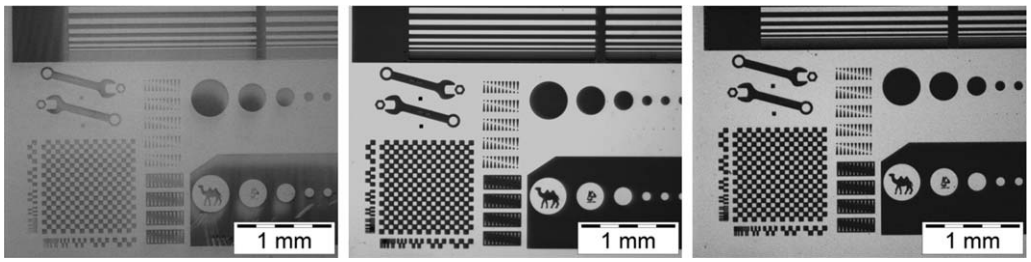

Figure 4. Green films produced out of sols with different initiator content (from left to right: 0.09, 0.45, 0.9 mmol) showing quality differences of films after development in organic solvent solution.

are used, the patterned green film structures smudge during development in the organic solvent mixture resulting in poor green film quality. Using higher initiator quantities (0.45, 0.9 mmol) causes smudge-proof structures. Exemplary patterned green films are shown in Figure 4. Green films made out of sols with higher initiator concentrations are crack free, fine patterned, and show good surface quality. The measured thicknesses of the films from low initiator quantities (0.09 mmol) were about 100–110 nm. Green films made out of both sols with higher initiator concentrations were more homogenous and had average thicknesses around 220 nm. During development with organic solvents films produced out of sols with less initiator were partly solved and, therefore, thickness was decreased by almost 50 % compared to films with higher initiator content. For films produced out of sols with higher initiator quantities (0.45, 0.9 mmol) an UV-dose around 5.4 J/cm^2 turned out to be sufficient for this patterning process. This UV-dose was chosen based on the gained knowledge of the PZT system.[20] Experiments with various UV-doses were not performed for the PST system. But corresponding tests were performed on the PZT system in our previous work, so some expectations can be given. Lower UV-dose should have the same negative effect on film quality like low initiator content due to a lower radical concentration and, therefore, insufficient polymerization reaction. Higher UV-dose should not change green film quality noticeably, because after a sufficient curing reaction there should not be a relevant improvement by extending the duration of the exposure. The UV-dose was calculated by multiplying lamp output and exposure time.

Ceramic Film Quality

Thin ceramic films with very low defect concentrations were obtained after thermal treatment of the green films. Figure 5 shows microscope pictures of the manufacturing process steps to the final ceramic micropatterned film. The first picture shows green film structures (left), the second picture (middle) shows the same film after debinding step (400°C, dwell time 1 h, heating-/cooling rate 5 K/min). The resulting ceramic film after the

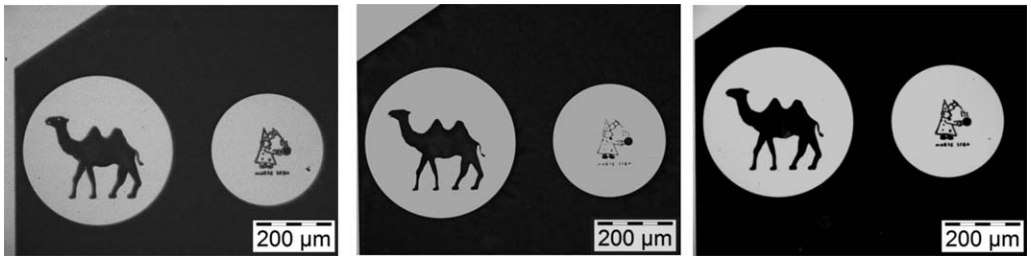

Figure 5. Microscope pictures illustrating the manufacturing process from green film (left), debinded film (middle) to sintered ceramic film (right).

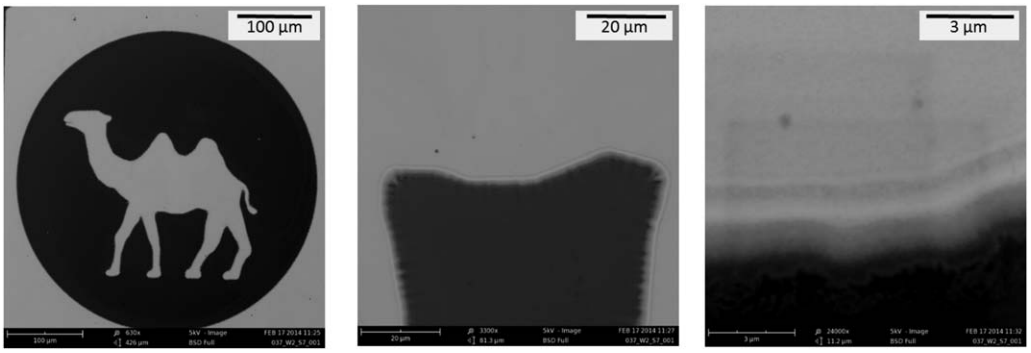

Figure 6. SEM photographs showing the high resolution of the process and the smooth surface morphology of the film.

final sintering step by rapid thermal annealing (650°C, dwell time 20 min, heating rate 50 K/s) is shown on the third picture (right). No significant lateral shrinkage was observed during thermal annealing.

Thin ceramic films with an average thickness of 80 nm, a lateral solution of 2–3 µm and only a few defects were produced successfully. A collection of micropatterned PST structures are shown in Figure 6. The films are polycrystalline and have a fine grained structure. The thickness of green xerogel and crystalline ceramic films was measured by profilometry. Average green film thickness was 220 nm and average ceramic film thickness was 80 nm. So volume shrinkage of the film during thermal treatment was about 64 vol %.

Thermal Decomposition Behavior

Dried powder of PST xerogel was investigated by Thermogravimetry and differential thermal analysis (TG/DTA)-measurement with the following temperature program. The oven was heated to a temperature of 80°C (heating rate: 5 K/min) and hold for 60 min, then heated to 400°C (heating rate: 5 K/min) and again hold for 60 min. A last heating step to 1200°C (heating rate: 5 K/min, 30 min) is added, and finally, the oven is cooled down to room temperature (cooling rate: 10 K/min).

During thermal treatment a five-step decomposition process of the dried gel powder was detected (see Figure 7). The first mass loss step of 6.5 wt % between 30 and 80°C indicates most likely the evaporation of organic compounds (e.g., ME and AA) of the gel. Mass loss of 12.1 wt % between 110 and 290°C combined with an exothermal DTA signal indicates the start of decomposition of organic compounds. The exothermal decomposition reaction reaches a maximum in the next mass loss step of 32.3 wt % up to 400°C, most likely caused by the loss of combustion products like water and carbon dioxide. This combustion is continued in the next mass loss step (2.4 wt %) up to 650°C. Until a temperature of 900°C is reached no further mass loss is detected. This last mass loss of 1.8 wt % at very high temperatures is most likely caused by the evaporation of volatile lead oxide. So loss of lead oxide is not a serious problem in this process because much lower temperatures are needed for the transformation of green films to the desired ceramic films with perovskite phase (see next section). Sun et al. published similar results for the thermal decomposition behavior of their PST-sol-gel systems.[29]

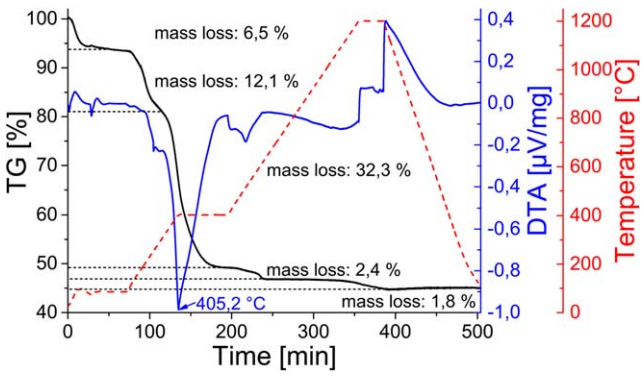

Figure 7. Thermogravimetry and differential thermal analysis of dried precursor sol. [Color figure can be viewed in the online issue, which is available at wileyonlinelibrary.com.]

Crystal Structure

Phase transition during thermal annealing of PST films to the desired perovskite phase was investigated by X-ray diffractometry (XRD) measurements. For these measurements samples of unstructured xerogel films were deposited on Si-substrates and annealed at various temperatures in the range of 400–650°C.

Crystal structure of the as-fired films was investigated by XRD technique. Figure 8 shows XRD-patterns of annealed, unstructured PST-films. The desired polycrystalline perovskite structure is formed at temperatures around 450°C below this temperature phase transition to the desired perovskite phase was not observed. The pleasantly low phase formation temperature made PST films obtained by this method interesting candidates for ferroelectric applications. Due to the low process temperatures it may be possible to use cheaper materials than high temperature compatible platinum or gold films as electrically conductive layers. Such materials may be silver or even aluminum.

Ferroelectric Properties

Ferroelectric properties of nonpolarized ceramic films were investigated by hysteresis measurements at room temperature. For first measurements samples of unstructured xerogel films were deposited on platinum plated Si-substrates and annealed at 650°C. As top electrodes small silver dots deposited by using silver lacquer were used. Preliminary results of nonoptimized thin films reveal ferroelectric behavior (see Figure 9). The

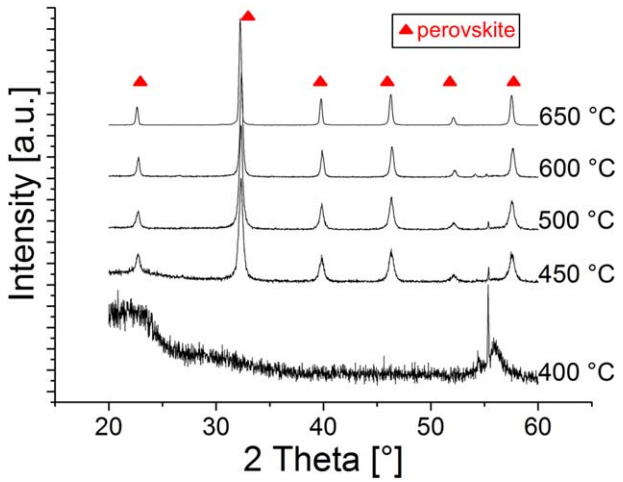

Figure 8. XRD patterns of PST films deposited on Si-substrates, annealed at 400°C (1 h, 5 K/min) and sintered at higher temperatures (450–650°C, 20 min, 50 K/sec). [Color figure can be viewed in the online issue, which is available at wileyonlinelibrary.com.]

shown hysteresis curve was measured after a pre-loop with the same settings. Obtained polarization values (remanent polarization $P_r = 0.02$ $\mu C/cm^2$) are smaller than previous reported measurements on thicker films.[8,12,15,30] PST films produced by chemical solution deposition methods with thicknesses around 400 nm showed remanent polarizations (P_r) between 1–2 $\mu C/cm^2$.[8,12,15] Films produced by physical vapor deposition methods like RF magnetron sputtering showed a remanent polarization of $P_r = 6$ $\mu C/cm^2$ [30] The polarization values of the PST films manufactured by direct UV-lithography might be improved by using a multilayer approach to obtain thicker films and by improving the electrical contact between the film and the top electrode. Deposition of a well-defined gold or platinum electrode by vacuum evaporation through a mask may be a better alternative to using silver lacquer. Detailed dielectric measurements (permittivity, polarization, tunability) on optimized samples and the investigation of temperature dependence of polarization and permittivity are either under investigation or at least planned for the near future. The results will be published later focusing on the dielectric properties of ceramic films produced by direct UV-lithography.

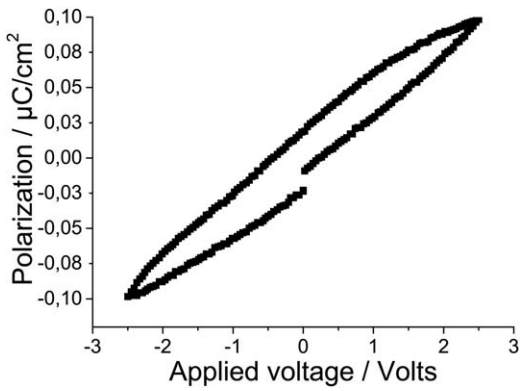

Figure 9. Hysteresis measurement of ceramic film deposited on platinum plated Si-substrate, annealed at 400°C (1 h, 5 K/min) and sintered at 650°C (20 min, 50 K/sec).

CONCLUSIONS

A polymer-based process for deposition and direct pattering of PST thin films by UV-lithography was demonstrated. Therefore, a photosensitive PST precursor sol which is acting as a negative photoresist was developed. The needed photosensitivity was achieved by chemical acrylic modification of the precursor sol and by addition of an UV-initiator to that sol. Photosensitive xerogel green PST films were obtained by spin coating and controlled drying. Induced by UV-light a polymerization reaction of acrylic acid-metal complexes takes place in irradiated areas of the green film. The resulting polymer-metal matrix is less soluble in organic solvents than not irradiated areas of the green film. This solubility change was applied to a patterning process by UV-lithography. Patterned green xerogel films were about 220 nm thick with minimum feature sizes in the low µm range (2–3 µm). These films were transferred to ceramic crystalline PST thin films by thermal annealing. The obtained perovskite thin films were almost defect free, fine grained and up to 80 nm thick. This process is an easy to handle and simple alternative to known methods for deposition and patterning of ferroelectric thin films. Due to the strict reduction to simple fabrications methods and renunciation of sophisticated techniques like the use of inert gas atmosphere or dehydrations steps, the process is an interesting alternative to other methods based on photosensitive sols. The developed sol system can be used like a standard negative photoresist and processed with existing clean room infrastructures and methods. Thicker ferroelectric films should be easily accessible with further affords, for example, multilayer approaches. Nonvolatile RAMs may be an interesting application for these PST thin films. Nevertheless film quality has to be optimized to improve the ferroelectric properties of the films. Further investigations of the dielectric properties of the films are under investigation and will be published later.

ACKNOWLEDGMENTS

The authors thank the state of Baden-Württemberg, "Ministerium für Wissenschaft, Forschung und Kunst", for financial support within the graduate school "Generierungsmechanismen von Mikrostrukturen" (GenMik).

REFERENCES

1. Muralt, P. J. *Micromech. Microeng.* **2000**, *10*, 136.
2. Anton, S. R.; Sodano, H. A. *Smart Mater. Struct.* **2007**, *16*, R1.
3. Jeon, Y. B.; Sood, R.; Jeong J.-h.; Kim, S.-G. *Sensors Actuators A* **2005**, *122*, 16.
4. Haertling, G. H. *J. Am. Ceram. Soc.* **1999**, *82*, 797.
5. Chung, H. J.; Chung, S. J.; Kim, J. H.; Woo, S. I. *Thin Solid Films* **2001**, *394*, 213.
6. Chung, H. J.; Kim, J. H.; Woo, S. I. *Chem. Mater.* **2001**, *13*, 1441.

7. Chun, Y.-H.; Fragkiadakis, C.; Bao, P.; Lüker, A.; Wright, R.; Hong, J.-S.; Kirby, P.; Zhang, Q.; Jackson, T.; Lancaster, M. J. Tunable Bandstop Resonator and Filter on Si-Substrate with PST Thin Film by Sol-Gel Deposition Microwave Conference, 2008. EuMC 2008. 38th European, **2008**, 13–16.
8. Sun, X.; Li, X.; Hou, S.; Huang, C.; Zou, J.; Li, M.; Peng, T.; Zhao, X.-Z. The effect of Mg doping on the dielectric and tunable properties of Pb0.3Sr0.7TiO3 thin films prepared by sol-gel method, *J. Appl. Phys. Part 1*, Springer-Verlag, **2013**, 1–7.
9. Lei, X.; Remiens, D.; Ponchel, F.; Soyer, C.; Wang, G.; Dong, X. *J. Am. Ceram. Soc.* **2011** *94*, 4323.
10. Chou, C.-C.; Hou, C.-S.; Chang, G.-C.; Cheng, H.-F. *Appl. Surf. Sci.* **1999**, *142*, 413.
11. Li, K.; Dong, X.; Remiens, D.; Lei, X.; Li, T.; Du, G.; Wang, G. *J. Am. Ceram. Soc.* **2013**, *96*, 1682.
12. Ponchel, F.; Lei, X.; Remiens, D.; Wang, G.; Dong, X. *Appl. Phys. Lett.* **2011**, *99*, 172905.
13. Pontes, F. M.; Leal, S. H.; Santos, M. R. M. C.; Leite, E. R.; Longo, E.; Soledade, L. E. B.; Chiquito, A. J.; Machado, M. A. C.; Varela, J. A. *Appl. Phys. A* **2005**, *80*, 875.
14. Li, X. T.; Huo, W. L.; Mak, C. L.; Sui, S.; Weng, W. J.; Han, G. R.; Shen, G.; Du, P. Y. *Mater. Chem. Phys.* **2008**, *108*, 417.
15. Kang, D. H.; Kim, J. H.; Park, J. H.; Yoon, K. H. *Mater. Res. Bull.* **2001**, *36*, 265.
16. Jain, M.; Majumder, S. B.; Guo, R.; Bhalla, A. S.; Katiyar, R. S. *Mater. Lett.* **2002**, *56*, 692.
17. Zhou, D.; Wu, W.; Jin, D.; Cheng, J.; Meng, Z. *IEEE Trans. Ultrason. Ferroelectr. Freq. Control.* **2008**, *55*, 1034.
18. Wang, D. G.; Chen, C. Z.; Liu, T. H. *Appl. Surf. Sci.* **2008**, *255*, 1637.
19. Leech, P. W.; Holland, A. S.; Sriram, S.; Bhaskaran, M. *Appl. Phys. A.* **2008**, *91*, 679.
20. Benkler, M.; Paul, F.; Schott, J.; Hanemann, T. Ferroelectric thin film fabrication by direct UV-lithography Microsystem Technologies, Springer Berlin Heidelberg, **2013**.
21. Tohge, N.; Takahashi, S.; Minami, T. *J. Am. Ceram. Soc.* **1991**, *74*, 67.
22. Faure, S.; Chaux, O.; Gaucher, P. *J. Phys. IV* **1998**, *8*, 69.
23. Uozumi, G.; Kageyama, K.; Atsuki, T.; Soyama, N.; Uchida, H.; Ogi, K. *Jpn. J. Appl. Phys. Part 1* **1999**, *38*, 5350.
24. Su-Min Ha, H.; Woo Sik Kim, H.; Hyung-Ho, P.; Tae Song Kim, H. *Ferroelectr. Lett. Sect.* **2002**, *273*, 351.
25. Marson, S.; Dorey, R.; Zhang, Q.; Whatmore, R. *Integr. Ferroelectr.* **2003**, *54*, 585.
26. Marson, S.; Dorey, R.; Zhang, Q.; Whatmore, RW.; Hardy, A.; Mullens, J. *J. Eur. Ceram. Soc.* **2004**, *24*,1925.
27. Kololuoma, T.; Hiltunen J.; Tuomikoski, M.; Lappalainen, J.; Rantala, J. P. In Soc. photo-opt. inst. (SPIE), conference on integrated optics-devices, materials and technology VIII 2004, 5355, pp 33–39.
28. Sumiyoshi, T.; Schnabel, W. *Makromol. Chem.* **1985**, *186*, 1811.
29. Sun, X.; Li, X.; Zhou, S.; Zhou, J. *Adv. Mater. Res.* **2010**, *148*, 887.
30. Fujii, T.; Du, J.; Karaki, T.; Adachi, M. J. *Korean Phys. Soc.* **2003**, *42*, 1178.